Linear Analysis of an Internal Seiche Generated at a Sharp Density Interface in a Shallow Lake with Varying Depth

Yō MIZUTA, Morimasa OHTANI and Isao YAKUWA
(Received June 30, 1987)

Abstract

A simple method to analyze, in the linear-wave approximation, an internal seiche generated at a sharp density-interface in a two-layer lake is shown. It is assumed that the shape of the lake is long, the lake has a rectangular cross-section with a shallow depth that varies. Starting with a set of hydraulic equations for a two-layer fluid model, wave equations for fast (surface) and slow (interface) modes are derived when the difference in density across the interface is small. The method to calculate eigen frequencies of the internal seiche numerically is also shown. The calculated results are compared with observational results at the thermocline of Kanayama Reservoir, and their coincidence is ascertained.

1. Introduction

It is well known that the various layers of different temperature, turbidity or salinity in a lake or reservoir can oscillate against one another because of the inhomogeneity in density. A stationary oscillation generated at the sharp density interface is called an internal seiche. Among theoretical treatments, the most appropriate one to analyze the internal seiche in the lake under investigation is chosen by the following criteria:

(a) Is the shape of the lake long or round?
(b) Is the shape of the cross-section rectangular or not? Is it uniform or not, along the long axis of the lake?
(c) Is the lake shallow or deep, in comparison with its horizontal size?
(d) Is the density interface sharp or vague?

When the lake is long and has a rectangular cross-section whose depth and width are uniform along its long axis, eigen frequencies of the internal seiche can be obtained in a compact form without restrictions of shallow water and/or sharp density interface.[1,2] On the other hand, when the cross-section varies along its long axis, some approximations are to be made.

The lake treated in this paper is assumed to have a long shape and a rectangular cross-section whose width is uniform but depth is varying. This is a model of a well-known type of lake which is created from naturally or artificially blocked rivers. When the depth is shallow compared with the length and the width of the lake, we can use the long-wave approximation. The lake is stratified in such a way that there is a sharp density interface but the difference in density across it is small. This makes it possible to adopt a two-layer fluid model and to simplify the equations by use of a small density ratio parameter $\varepsilon = 1 -$

Department of Engineering Science, Faculty of Engineering, Hokkaido University, Sapporo 060, Japan

ρ_1/ρ_2, where ρ_1, ρ_2 are the density of the upper and the lower layer. Thus, reduced wave equations for fast (surface) and slow (interface) modes are derived, as shown in section 2. In order to calculate numerically the eigen frequencies of the internal seiche, the wave equation for the slow mode is transformed into a set of algebraic eigenvalue equations under some boundary conditions. This process is shown in section 3. In section 4, calculated eigen frequencies are compared with the positions of some peaks in a power spectrum of an isotherm varying in time, which was observed at Kanayama Reservoir in the summer of 1985.

2. Wave Equations for Fast and Slow Modes

We consider here the seiche with a long wavelength and a small amplitude, which is generated at the interface of a two-layer lake. Its cross-section is rectangular, and the width is uniform from cross-section to cross-section, but its bottom is inclined from the upper end toward the lower as shown in Fig. 1. Assuming that the fluids in both layers are

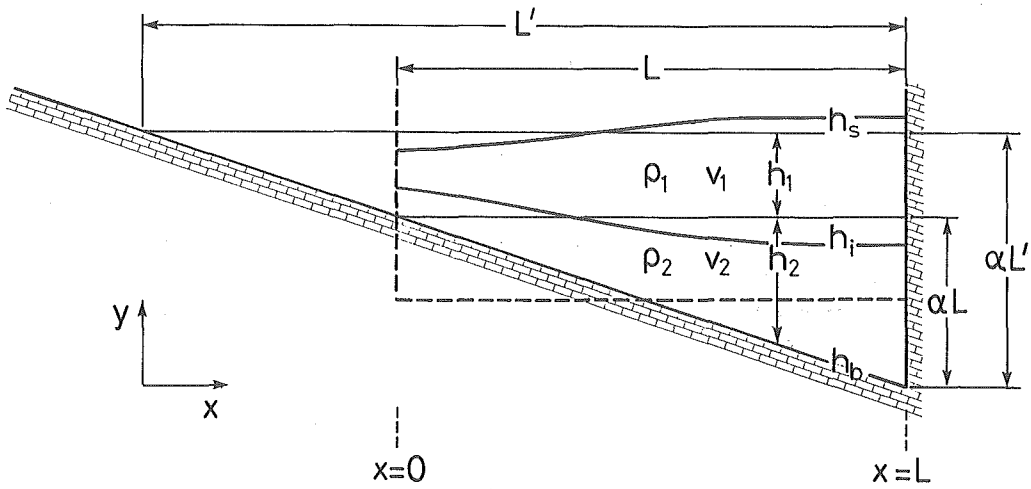

Fig. 1 Definition sketch of a two-layer lake with an inclined bottom. A basin shown by broken lines is used to model the lake more simply.

inviscid and incompressible, we start with the following hydraulic equations in the linear-wave approximation in each layer : [3]

$$\frac{\partial (h_s - h_1)}{\partial t} + \frac{\partial [v_1 (h_s - h_1)]}{\partial x} = 0, \tag{1}$$

$$\frac{\partial v_1}{\partial t} + g\frac{\partial h_s}{\partial x} = 0, \tag{2}$$

$$\frac{\partial (h_1 - h_b)}{\partial t} + \frac{\partial [v_2 (h_1 - h_b)]}{\partial x} = 0, \tag{3}$$

$$\frac{\partial v_2}{\partial t} + g\frac{\partial [(1-\varepsilon) h_s + \varepsilon h_1]}{\partial x} = 0, \tag{4}$$

where $h_s(x, t)$, $h_i(x, t)$, $h_b(x)$ are the height of the surface, interface and bottom, and $v_1(x, t)$, $v_2(x, t)$ are the mean flow velocity of the upper and lower layer. In eqs. (2) and (4), such nonlinear terms as $\partial v_2^2/\partial x$ are already neglected.

Boundary conditions in the present problem are

$$h_s = \text{finite}, \quad h_i = \text{finite} \quad \text{at } x = 0, \tag{5), (6}$$

$$(h_s)_x = 0, \qquad (h_i)_x = 0 \qquad \text{at } x = L. \tag{7), (8}$$

Next, we eliminate v_1 and v_2 from eqs. (1)–(4). Then, the terms $v_1\partial(h_s - h_i)/\partial t$ and $v_2\partial(h_i - h_b)/\partial t$ are neglected, and $(h_s - h_i)\partial v_1/\partial t$ and $(h_i - h_b)\partial v_2/\partial t$ are replaced by $h_1\partial v_1/\partial t$ and $h_2\partial v_2/\partial t$, respectively, owing to the linear-wave approximation, where $h_1 \equiv h_s - h_i$, $h_2 \equiv h_i - h_b$ are the thickness of the upper and lower layer when both the surface and the interface are quiescent.

Consequently,

$$\frac{\partial^2(h_s - h_i)}{\partial t^2} - gh_1\frac{\partial^2 h_s}{\partial x^2} = 0, \tag{9}$$

$$\frac{\partial^2 h_i}{\partial t^2} - g\frac{\partial}{\partial x}\left(h_2\frac{\partial[(1-\varepsilon)h_s + \varepsilon h_i]}{\partial x}\right) = 0. \tag{10}$$

In the case that h_2 is uniform, it is readily shown that eqs. (9) and (10) have a fast mode (denoted by (+)) and a slow mode (denoted by (−)). First, $h_s = \tilde{h}_s \cdot \exp[ik(x - ct)]$ and $h_i = \tilde{h}_i \cdot \exp[ik(x - ct)]$ are used in eqs. (9) and (10), where k is the wavenumber and c is the phase velocity. Second, the eigenvalue problem is solved, in which eigenvalue is c and the elements of eigenvector are $\tilde{h}_s$ and $\tilde{h}_i$. Then, within the confines of $\varepsilon \to 0$, the phase velocity and the ratio between $\tilde{h}_s$ and $\tilde{h}_i$ of each mode are shown to be

$$\tilde{h}_s^{(+)}/\tilde{h}_i^{(+)} = (h_1 + h_2)/h_2 \qquad \text{for } [c^{(+)}]^2 = g(h_1 + h_2), \tag{11}$$

$$\tilde{h}_s^{(-)}/\tilde{h}_i^{(-)} = -\varepsilon h_2/(h_1 + h_2) \quad \text{for } [c^{(-)}]^2 = \varepsilon g(1/h_1 + 1/h_2)^{-1}. \tag{12}$$

In order to derive the reduced wave equations for each mode which holds also in the case of varying depth, we use

$$h_s = h_s^{(+)} + \varepsilon h_s^{(-)}, \quad \text{where} \begin{cases} h_s^{(+)} = O(\varepsilon^0), & (h_s^{(+)})_{tt} = O(\varepsilon^0), \\ h_s^{(-)} = O(\varepsilon^0), & (h_s^{(-)})_{tt} = O(\varepsilon^1), \end{cases} \tag{13}$$

$$h_i = h_i^{(+)} + h_i^{(-)}, \quad \text{where} \begin{cases} h_i^{(+)} = O(\varepsilon^0), & (h_i^{(+)})_{tt} = O(\varepsilon^0), \\ h_i^{(-)} = O(\varepsilon^0), & (h_i^{(-)})_{tt} = O(\varepsilon^1), \end{cases} \tag{14}$$

in (9) and (10). Equations (11) and (12) give us a clue for determining the magnitude of $h_s^{(+)}$, $h_i^{(+)}$, $h_s^{(-)}$, and $h_i^{(-)}$ themselves and their time derivatives with respect to ε.

Equations for the fast mode are obtained from eqs. (9) and (10) at the order of ε^0:

$$(h_s^{(+)})_{tt} - (h_i^{(+)})_{tt} - gh_1(h_s^{(+)})_{xx} = 0, \tag{15}$$

$$(h_i^{(+)})_{tt} - g[h_2(h_s^{(+)})_x]_x = 0, \tag{16}$$

and the sum of them gives the wave equation for the fast mode

$$(h_s^{(+)})_{tt} - g[(h_1 + h_2)(h_s^{(+)})_x]_x = 0. \tag{17}$$

Once $h_s^{(+)}$ is known, $h_i^{(+)}$ is given by integrating eq. (16).

On the other hand, equations for the slow mode are derived from eqs. (9) and (10) at the order of ε^1:

$$-(h_i^{(-)})_{tt} - \varepsilon gh_1(h_s^{(-)})_{xx} = 0, \tag{18}$$

$$(h_1^{(-)})_{tt} - \varepsilon g[h_2(h_s^{(-)} + h_1^{(-)})_x]_x = 0. \tag{19}$$

By summing up (18) and (19), and considering $(h_s^{(-)})_x = (h_1^{(-)})_x = 0$ from the boundary conditions (7) and (8), we have a relation

$$(h_s^{(-)})_x = -[h_2/(h_1 + h_2)]\,(h_1^{(-)})_x. \tag{20}$$

Equation (20) indicates that the oscillations of the surface and the interface are in an antiphase state to each other. If eq. (20) is used, the wave equation for the slow mode is obtained from eq. (18) as

$$(h_1^{(-)})_{tt} - \varepsilon g[(1/h_1 + 1/h_2)^{-1}(h_1^{(-)})_x]_x = 0. \tag{21}$$

3. Method of Numerical Calculation

Eigen frequencies of the internal seiche are obtained from eq. (21) under the boundary conditions (6) and (8). Here we assume that h_2 varies as αx, where α is the inclination of the bottom, and we put $h_1^{(-)}(x, t) = Y(x)\exp(i\sigma t)$, where σ is the frequency. Furthermore, we define ω and z as $\omega = \sigma/[\sqrt{\varepsilon g h_1}(\alpha/h_1)]$ and $z = 2\omega\sqrt{\alpha x/h_1}$. Then eqs. (21), (6) and (8), where h_1 is replaced by $h_1^{(-)}$, are rewritten as follows:

$$\left(\frac{z}{1+(z/2\omega)^2}Y_z\right)_z + zY = 0, \tag{22}$$

$$Y = \text{finite} \quad \text{at } z = 0, \tag{23}$$

$$Y_z = 0 \qquad \text{at } z = 2\omega\sqrt{\alpha L/h_1} \equiv Z. \tag{24}$$

Since eq. (22) is reduced to the Bessel differential equation of the zeroth order when $z \ll 2\omega$, we can expand Y, insofar as αL is not too large compared with h_1, into a series of orthonormal functions

$$Y(z) = \sum_{n=1}^{\infty} c_n \phi_n(z), \tag{25}$$

$$\phi_n(z) \equiv \sqrt{h_1/2\alpha L}\; J_0(\lambda_n z/Z)/|J_0(\lambda_n)|, \tag{26}$$

where J_0 is the Bessel function of the zeroth order, and λ_n's are the roots of equations $J_0'(z) = -J_1(z) = 0$. Function $Y(z)$ given by (25) satisfies the boundary conditions (23) and (24) since each $\phi_n(z)$ does. On numerical calculation, the infinite sum in eq. (25) is truncated at the N-th term where N is a large integer.

If both sides of eq. (22) are multiplied by $\phi_m(z)$ $(m = 1, N)$ and integrated from 0 to Z with respect to z, the following set of algebraic eigenvalue equations are obtained:

$$\sum_{n=1}^{N}(-A_{mn} + \delta_{mn}\omega^2)c_n = 0 \quad (m = 1, N), \tag{27}$$

$$A_{mn} = \frac{\lambda_m\lambda_n}{|J_0(\lambda_m)J_0(\lambda_n)|}\frac{h_1}{2\alpha L}\int_0^1 dz\,\frac{J_1(\lambda_m z)\,zJ_1(\lambda_n z)}{1+(\alpha L/h_1)z^2}. \tag{28}$$

Note that A_{mn} is symmetric with respect to m and n, and includes only $\alpha L/h_1$ as a parameter where αL is the value of h_2 at the lower end of the lake. Thus, ω^2 is real and it depends only on $\alpha L/h_1$. Since each eigen frequency of the internal seiche is obtained from $\sigma = \sqrt{\varepsilon g h}(\alpha/h_1)\omega$, parameters necessary to determine σ are N, h_1, αL, α, ε and g in all.

4. Comparison Run against the Results of Observation

As an example, the eigen frequencies of the internal seiche at the thermocline of Kanayama Reservoir were calculated, and they were compared with the observational results.[4] Kanayama Reservoir, which was constructed in 1966 by blocking the Sorachi River, is located around the center of Hokkaido. It has an elongated shape with a length L' of about 10km, and a width of less than 1km. The bottom inclines almost uniformly and the average inclination α is 0.0037. Results shown here were observed during a period from 9th to 18th of August in 1985 when the thermocline in the reservoir was prominent. The total depth of the water at the dam ($\alpha L' = h_1 + \alpha L$) was 37m on an average during this period.

The water temperature was measured at three stations in the reservoir, namely, near the dam (Sta. 1), at the railway bridge (Sta. 2, 3.8km upstream from the dam) and at the Shikagoe Bridge (Sta. 3, 7.3km upstream from the dam). At Stations 1 and 3, thermisters were set at every 0.5m from the surface to the depth of 5.0m, at every 1.0m from 5.0m to 10.0m and at every 2.0m from 10.0m to the bed. At Sta. 2, thermisters were set beneath the surface, at the depth of 1.0m, 3.0m, 3.75m, 5.0m, and at the bottom. The data from 21 thermisters at Sta. 1 and those from 18 thermisters at Sta. 3 were recorded on hybrid recorders every 30 minutes. At Sta. 2, the data was recorded on a memory recorder every 30 minutes.

Two sets of figures were produced from the records of water temperature. One set of figures are vertical distributions of water temperature at each station every 6 hours. Figure 2 is one of those observed at Sta. 1 at 6 o'clock on August 12. From this figure, the thickness of the upper layer h_1 and the density ratio parameter ε can be estimated, and their values during the above-mentioned period are $h_1 = 2.0 \sim 4.5$m and $\varepsilon = 0.0016 \sim 0.0026$. Another set of figures are power spectra of temporally changing elevation of each isotherm at each station. Figure 3 shows the spectrum of the 14°C isotherm at Sta. 1 during the period. The elevation of each isotherm is calculated by interpolation from the recorded water temperature at each depth. Eigen frequencies of the internal seiche are known from this spectrum.

The three lowest eigen frequencies calculated by the present method (this case is denoted by I) are shown as functions of varying h_1 and ε by solid lines in Fig. 4. The eigen frequencies calculated under $h_1 = 2.8$m and $\varepsilon = 0.0021$ are shown by arrows in Fig. 3, and they are ascertained to agree with the positions of the three prominent peaks in the spectrum. The value of ε in this case corresponds to the difference in temperature between 8°C and 22°C. Function $Y(z)$ in eq. (25) is approximated by 10 orthonormal functions, and the convergence is sufficient for the three lowest eigen frequencies.

When the reservoir is replaced by a simpler basin with a vertical wall at $x = 0$ and with a constant depth of $h_2 = \alpha L/2$, as shown by broken lines in Fig. 1, eigen frequencies are given by $\sigma = \sqrt{\varepsilon g/(1/h_1 + 1/h_2)}(n\pi/L)$ where n is an integer (this case is denoted by II). The values due to this equation are also shown by broken lines in Fig. 4 for comparison. It is seen that the eigen frequencies in the case I are shifted toward the lower frequency in comparison with those in the case II, and this tendency is enlarged for higher order eigen frequencies. At Kanayama Reservoir, the difference between cases I and II is only of the

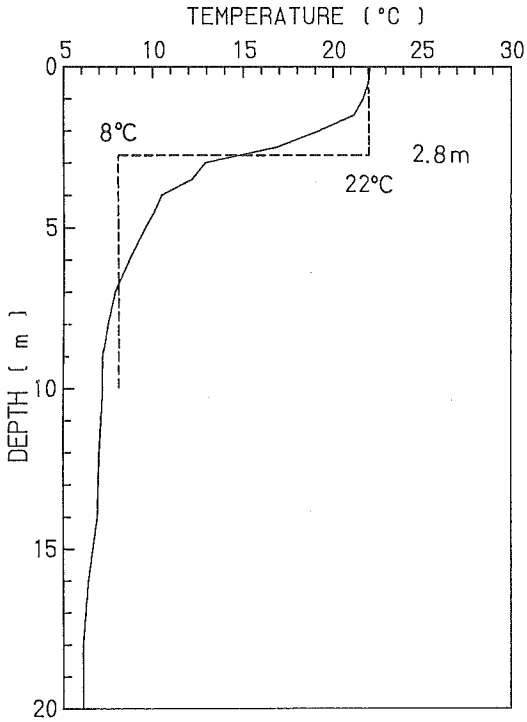

Fig. 2 Measured vertical distribution of water temperature at Sta. 1 at 6 o'clock of August 12, 1985. Such distribution as shown by broken lines is instead used on calculation.

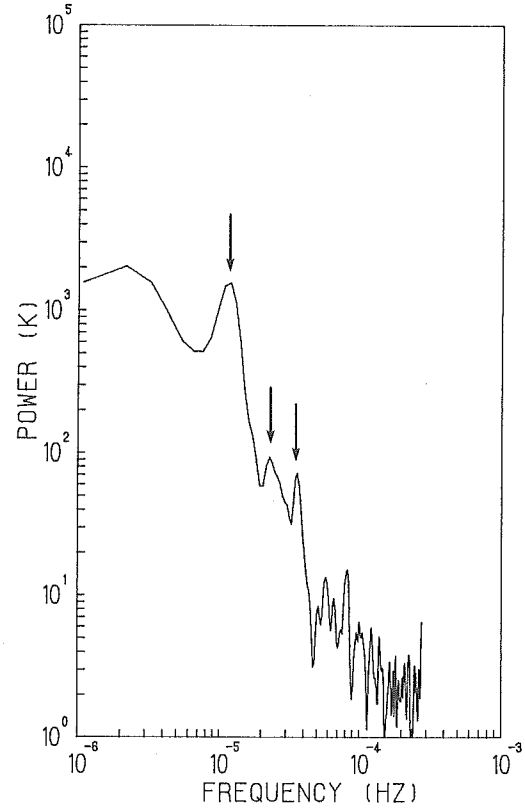

Fig. 3 Spectrum of the elevation of the 14°C isotherm at Sta. 1. Arrows show the values of the three lowest eigen frequencies calculated under $h_1 = 2.8$m, $\alpha L = 34.0$m, $\alpha = 0.0037$ and $\varepsilon = 0.0021$.

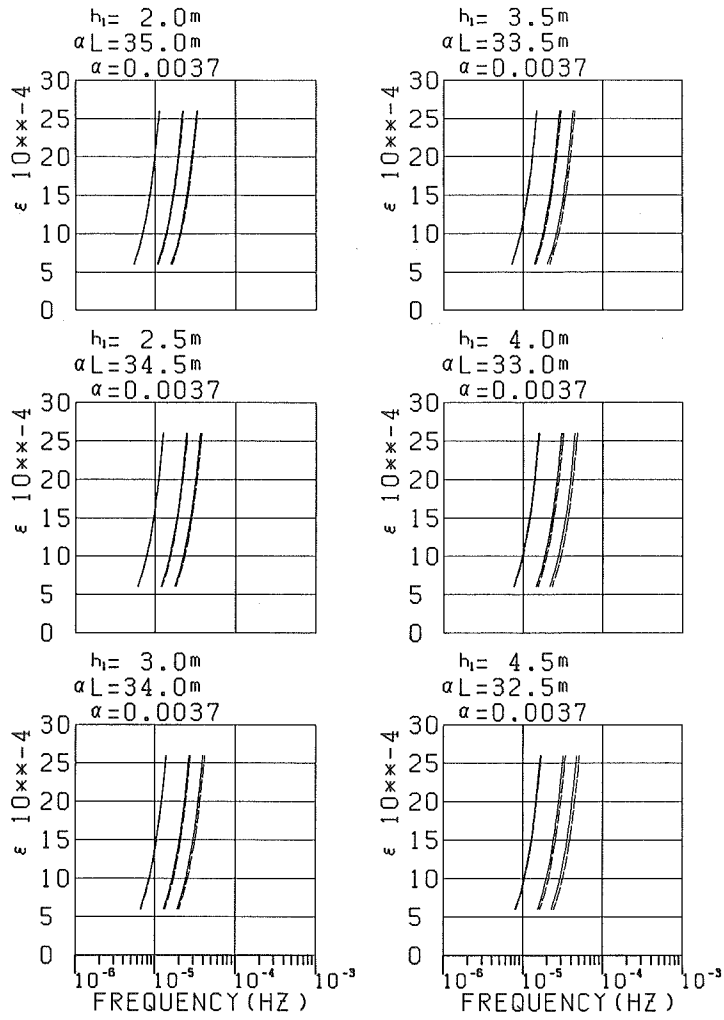

Fig. 4 The three lowest eigen frequencies calculated as functions of h_1 and ε under $h_1+\alpha L=37.0$m and $\alpha=0.0037$. Broken lines show the eigen frequencies in a simpler basin in **Fig. 1**.

same order of the range of accuracy in the observation, but it can be larger at the lake where the inclination of the bottom is larger than that of Kanayama Reservoir.

5. Conclusion

A theoretical approach to obtain eigen frequencies of an internal seiche at a sharp interface in a lake with varying depth is presented. Results of numerical calculation for Kanayama Reservoir can explain the observational results. Although eigen frequencies

calculated by the present method differ only slightly from those by the fore-existing method in Kanayama Reservoir, the differences between them are expected to be enlarged in other lakes.

Acknowledgement

The authors wish to express their gratitude to the Hokkaido Development Bureau for supplying valuable data. They also thank to Mr. Keiji Okamura, graduate student of Hokkaido University, for his assistance in measuring and arranging the data in the course of this study. Numerical calculations were made by HITAC M-680H at Hokkaido University Computing Center. A package of codes NUMPAC offered by Nagoya University Computing Center was used in solving the eigenvalue problem.

References

1) Phillips, O.M.: The dynamics of the upper ocean (Cambridge University Press, London, 1977) 2nd ed., p. 206.
2) Lamb, H.: Hydrodynamics (Cambridge University Press, London, 1932) 6th ed., p. 372.
3) Schijf, J.B. and Schönfeld, J.C.: Theoretical consideration on the motion of salt and fresh water, Proc. of Minnesota International Hydraulic Convention, IAHR and ASCE, 1953, p. 321.
4) Ohtani, M., Okamura, K. and Yakuwa, I.: Wind forced waves in a stratified reservoir, 22nd International Congress, IAHR, Lausanne, 1987.